From Newton's second law to Huygens's principle: visualizing waves in a large array of masses joined by springs

2009 Eur. J. Phys. 30 1217

(http://iopscience.iop.org/0143-0807/30/6/002)

IOP PUBLISHING EUROPEAN JOURNAL OF PHYSICS

Eur. J. Phys. **30** (2009) 1217–1228 doi:10.1088/0143-0807/30/6/002

From Newton's second law to Huygens's principle: visualizing waves in a large array of masses joined by springs

A E Dolinko

Instituto de Física Rosario (CONICET-UNR), Bv. 27 de Febrero 210 Bis, 2000 Rosario, Argentina
and
Departamento de Física, Facultad de Ciencias Exactas, Ingeniera y Agrimensura, Universidad Nacional de Rosario, S2000BTP Rosario, Argentina

E-mail: andres.eze.d@gmail.com

Received 11 May 2009, in final form 16 July 2009
Published 8 September 2009
Online at stacks.iop.org/EJP/30/1217

Abstract

By simulating the dynamics of a bidimensional array of springs and masses, the propagation of conveniently generated waves is visualized. The simulation is exclusively based on Newton's second law and was made to provide insight into the physics of wave propagation. By controlling parameters such as the magnitude of the mass and the elastic constant of the mesh elements, it was possible to change the properties of the medium in order to observe the characteristic phenomena of wave mechanics, such as diffraction and interference. Finally, several examples of waves propagating in media with different configurations are presented, including the application of the simulation to the study of frequency response of a complex structure.

M This article features online multimedia enhancements

1. Introduction

There exist two ways of describing the nature in physics. One is through the concept of particles which is based on the idea of trajectory and is described by Newton's laws in classical mechanics. On the other hand, certain phenomena are better described by means of the concept of waves. The concept of particles is, in principle, opposite to the concept of waves since the first one refers to a localized entity while the second one refers to an entity whose description takes sense when an extended region of space is considered. The wave phenomena are well described by Huygens's principle, in which it is stated that the wavefront

of a propagating wave at any instant conforms to the envelope of spherical wavelets emanating from every point on the wavefront at the prior instant and it seems to be irreconcilable with the image of trajectory. However, it appears that there exists an underlying relationship between both formalisms [1].

One demonstration of this underlying connection is shown in this work, in which a simulation of the phenomenon of wave propagation is presented on the basis of the description of a bidimensional array of masses linked by springs. No wave equation is included *a priori*, and Newton's second law exclusively governs the system. The waves are generated by an adequate excitation of the masses and they propagate through the entire space of simulation. It is verified that the generated waves respond accurately to the behaviour predicted by Huygens's principle. Moreover, the known phenomena of wave mechanics, such as reflection and refraction, are also observed.

The proposed simulation allows observing the movement of the array of masses at the same time it is running. Consequently, the evolution of the wavefronts corresponding to the collective movement of the masses can be clearly visualized. Therefore, this work is intended for undergraduate students of physics or engineering, who may find the proposed simulation particularly useful since it permits insight into the dynamics of wave propagation to be obtained. Although several works on simulations of wave propagation have been reported [2–4], the present work has the advantage of being based on a very simple and intuitive algorithm that can be implemented by students to observe and visualize the dynamics of mechanical waves. Consequently, the proposed approach could represent a valuable tool in the field of physics education.

The characteristics and the size of the simulation space are easily determined by a set of digital pictures with the same size in pixels. A similar approach was also implemented in [5] to determine the medium characteristics in a simulation of heat propagation. The pictures define bitmaps in which each pixel corresponds to the location of a mass element of the array. In this manner, the number of masses in the array is automatically established by the size of the picture. The grey level of the pixels in each bitmap codes the magnitude of a physical characteristic of the corresponding mass element in the array. One of the bitmaps codes the mass value of the elements, and therefore, the grey level of each pixel will be proportional to the mass value of the corresponding array element. A second bitmap codes the value of the damping for the corresponding mass and a third bitmap codes the magnitude of the force externally applied to it. Since these pictures can easily be generated by means of any photo-editor program, the dynamics of the waves propagating in any bidimensional structure can easily be visualized and studied.

2. The physical model

The model consists in a bidimensional array of $p \times q$ masses contained in the **x**–**y** plane and joined to their four nearest neighbours by means of elastic springs separated by a distance d. The movement of each mass is constrained to the **z**-axis, that is, to the direction that is normal to the plane formed by the bidimensional array. The net force on each mass is null when all the masses are at rest and their **z** coordinate is zero. Therefore, the system is in equilibrium under these conditions. In order to generate a transversal wave, an external force along the **z**-axis is applied on the masses to be excited. When this is made on one of the masses of the array, it is separated from the equilibrium and a restoring force generated by the neighbouring masses appears. Due to Newton's action–reaction principle, these forces also displace the neighbouring masses from the equilibrium and this movement propagates away through the entire set of masses, generating the wave.

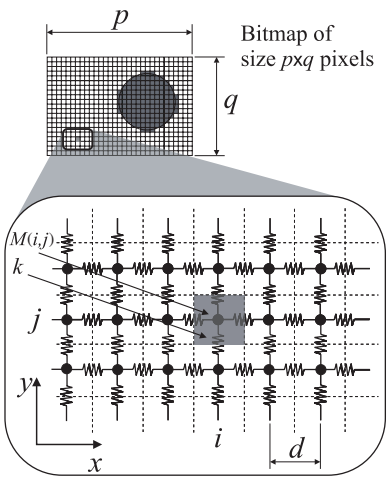

Figure 1. Interpretation of the bitmap M.

In the limit $p, q \to \infty$, the array of masses can be considered as a continuous medium representing an elastic membrane of any shape, homogeneously stretched with a tension $T = F_e/l_T$ and a superficial density mass $\mu = mN_m/s$, where F_e is the elastic force, l_T is the transversal section, which in this case is one dimensional and corresponds to a longitude, m is the mass of the mesh element and N_m is the number of masses per unit area s. The speed of the waves in the elastic membrane will be $v = \sqrt{T/\mu}$. If we consider the medium with a given superficial density mass being the ground level, the waves will have the maximum speed in this region and lower speed in regions with higher superficial density mass. In this manner, the waves travelling through regions of different superficial density mass will behave like light waves travelling through regions with a different refraction index. If the masses at the ground level region have a value m_0 and the waves travel here with speed v_0, the refraction index will be

$$n_R = \frac{v_0}{v} = \sqrt{\frac{m}{m_0}}, \tag{1}$$

where $v < v_0$ is the speed of the waves in the regions with a value of mass $m > m_0$.

3. Description of the simulation

The simulation begins by defining a bidimensional space that is determined by a digital picture or bitmap M with a size of $p \times q$ pixels. The bitmap defines a matrix with coordinates (i, j) contained in the **x**–**y** plane with $i = 1, 2, \ldots, p$ and $j = 1, 2, \ldots, q$. The elements (i, j) of the matrix determine the position of oscillating masses separated by a distance d measured in meters and joined by springs of elastic constant k so that each pixel in the bitmap represents a mass and the grey level, ranging from 0 to 255, codes its magnitude. A second bitmap D of the same size as M codes in grey levels the damping constant of the corresponding mass. In this manner, an array of $p \times q$ masses, each one with a magnitude $M(i, j)$, a damping constant $D(i, j)$, and joined by springs of elastic constant k is defined, as is shown in figure 1.

An additional bitmap E with a size of $p \times q$ pixels defines the masses that will be excited by the application of an external force. The grey levels in this bitmap determine the magnitude

of the external force applied on each mass. In this case, a grey level of 128 indicates that no force is applied on the mass. On the other hand, grey levels with a value over 128 are interpreted as a positive force and grey levels with a value under 128 are interpreted as a negative force.

The next step consists in defining the physical constants of the model. It is necessary to convert the values of mass, damping constant and externally applied force coded in grey levels to adequate physical units. Therefore, three matrices M_{phys}, D_{phys} and E_{phys} of size $p \times q$ containing the physical values of mass, damping constant and externally applied force are defined. These matrices are related to M, D and E as follows:

$$M_{\text{phys}} = m_0 + Mm_p, \tag{2}$$

$$D_{\text{phys}} = D\mu_p, \tag{3}$$

$$E_{\text{phys}} = r_p(E - 128), \tag{4}$$

where m_0 in (2) is a ground level mass, which is included to avoid the existence of a zero mass element producing infinite acceleration if the corresponding grey level becomes zero. The proportionality constant m_p in (2) has units of (kg/grey level) and the constant μ_p in (3) has units of (N s/m/grey level. r_p in (4) is a proportionality constant with units of (N/grey level) that converts the value of grey level provided by the bitmap E to a value of force. The elastic constant k has already been defined, and it is the same for all the elements. We define a set of additional matrices of size $p \times q$ to store the dynamic variables of each mass. $H(i, j)$, $V(i, j)$, $A(i, j)$ and $F(i, j)$ will store the normal displacement, speed, acceleration and total applied force on each mass located at the coordinate (i, j). Additionally, we also define a set of auxiliary matrices of the same size called $F_x^{(-)}(i, j)$, $F_x^{(+)}(i, j)$, $F_y^{(-)}(i, j)$, $F_y^{(+)}(i, j)$ to store the forces on the mass located at (i, j) due to the neighbour masses located at $(i - 1, j)$, $(i + 1, j)$, $(i, j - 1)$ and $(i, j + 1)$, respectively.

In analogy with optics, the intensity of the collective movement of the masses will be calculated by integrating the square of the displacements of each mass, to give a diagram of the intensity distribution of the waves. The intensity will be stored in a matrix $I(i, j)$.

4. Running the simulation

The simulation consists in an algorithm that begins by sweeping all the elements of the matrices of size $p \times q$ from left to right and from up to down to refresh the dynamic variables during an integer number of loops n. We suppose that the applied force on each mass determined by the bitmap E varies harmonically over time so that

$$E_t = E_{\text{phys}} \sin(\omega\tau n + \varphi), \tag{5}$$

where E_t is the harmonically varying external force applied, ω is the angular frequency of the excitation, φ is the initial phase of the harmonic excitation and τ is an adapting constant with units of (s/loop cycle) that converts the number of loop cycles to a variable with units of time, and therefore, the product τn represents the discretized time variable. On the other hand, the product $\omega\tau$ in the expression (5) should be smaller than π in order to fulfil the Nyquist–Shannon sampling theorem that states a criterion in which the frequency of signal sampling must be at least twice the highest signal frequency component. In our case, the sinusoidal wave form of the externally applied force with period 2π should be sampled at twice its frequency, that is, with a period of π or shorter every loop cycle n. This criterion basically ensures that the alternating nature of the external excitation is preserved after the sampling.

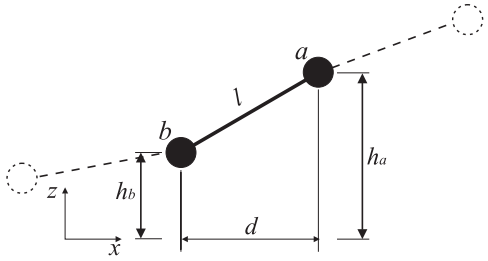

Figure 2. Elastic force between the masses.

Due to the fact that in general few masses are excited to generate wavefronts with a simple symmetry (i.e., circular or plane waves), the matrix E will be generally a mask with all the pixels in grey (null applied force) and those pixels to be excited in white (positive applied force) or black (negative applied force).

The next step consists in calculating the total force on each mass. The total force includes the applied external force E_t, the damping force F_{damp} and the elastic force applied by the four neighbouring masses given by matrices $F_x^{(-)}(i, j)$, $F_x^{(+)}(i, j)$, $F_y^{(-)}(i, j)$ and $F_y^{(+)}(i, j)$. So the total force for the mass located at (i, j) can be expressed as

$$F(i, j) = E_t(i, j) + F_x^{(-)}(i, j) + F_x^{(+)}(i, j) + F_y^{(-)}(i, j) + F_y^{(+)}(i, j) + F_{\text{damp}}(i, j). \tag{6}$$

The damping force is given by

$$F_{\text{damp}}(i, j) = D_{\text{phys}}(i, j) * V(i, j), \tag{7}$$

where the matrix multiplication is a point-to-point multiplication, each element of D_{phys} being multiplied by its corresponding element of V.

The modulus of the elastic force F_e on a mass a due to a neighbour mass b is given by

$$|F_e| = |k(l - l_0)|, \tag{8}$$

where l is the separation between the masses and l_0 is the natural length of the spring. The masses move only in the **z**-direction that is normal to the plane of the array so that the component in the **z**-direction is obtained by projecting (8) and results in

$$F_e = k(l - l_0)\frac{h_b - h_a}{l}, \tag{9}$$

where $h_{a,b}$ are the positions of the masses along **z** (see figure 2). Now, we make the approximation in which the strings are prestretched and where $l_0 \to 0$ [1]. In this manner, the elastic force can be approximated as

$$F_e = k(h_b - h_a). \tag{10}$$

Consequently, the forces $F_x^{(-)}(i, j)$, $F_x^{(+)}(i, j)$, $F_y^{(-)}(i, j)$ and $F_y^{(+)}(i, j)$ on the mass located at (i, j) due to the neighbour masses located at $(i - 1, j)$, $(i + 1, j)$, $(i, j - 1)$ and $(i, j + 1)$ are calculated in terms of the previously defined matrices as

$$F_x^{(-)}(i, j) = k(H(i - 1, j) - H(i, j)) \tag{11}$$

$$F_x^{(+)}(i, j) = k(H(i + 1, j) - H(i, j)) \tag{12}$$

$$F_y^{(-)}(i, j) = k(H(i, j - 1) - H(i, j)) \tag{13}$$

$$F_y^{(+)}(i, j) = k(H(i, j + 1) - H(i, j)). \tag{14}$$

(a) (b) (c)

Figure 3. Definition of the simulation space: (a) density mass, (b) excitation and (c) damping.

By means of Newton's second law, we calculate the acceleration matrix A determining the acceleration of each mass. This matrix is computed as

$$A(i, j) = F(i, j)/M_{\text{phys}}(i, j), \tag{15}$$

where the matrix division is a point-to-point division, each element of F being divided by its corresponding element of M_{phys}.

The speed matrix V is obtained by integrating the acceleration. In this manner, the values of the speed matrix $V(n-1)$ in the previous loop cycle $(n-1)$ are refreshed for the present loop cycle as

$$V^{(n)}(i, j) = V^{(n-1)}(i, j) + A^{(n)}(i, j). \tag{16}$$

The new displacement matrix H is also obtained by refreshing as

$$H^{(n)}(i, j) = H^{(n-1)}(i, j) + V^{(n)}(i, j). \tag{17}$$

The intensity is calculated by integrating the square of the displacement matrix as

$$I^{(n)}(i, j) = I^{(n-1)}(i, j) + (H^{(n)}(i, j))^2. \tag{18}$$

In this point, the integer variable n is incremented by 1, and all the simulation cycle is repeated from equation (5).

5. Examples

5.1. Visualizing the wave dynamics

Figure 3(a) shows a bitmap M with a size of 200 × 200 pixels that gives the density mass distribution and defines the simulation space. The separation among the masses is $d = 1$ mm so that the simulation space represents a real space of 20 × 20 cm^2. The bitmap shows a circle in grey, corresponding to a region of different refraction index in relation to the rest of the medium, in black. The region in black has a ground density mass $\mu_0 = 1$ kg m^{-2} and the circle has a density mass $\mu = 1.7$ kg m^{-2}. Therefore, according to (1) the equivalent refraction index of the circle is approximately $n_R = 1.3$. The elastic constant was set to $k = 0.3$ N m^{-1}. Figure 3(b) shows the bitmap E that indicates the masses to be excited harmonically, which in this case are those contained in a vertical line on the left side of the bitmap, in white. In this manner, a plane wave travelling from the left to the right of the simulation space will be generated. The frequency of the harmonic excitation was set to $\omega = 250$ rad s^{-1} and the adapting constant, which was defined in (5), was set to $\tau = 1$ ms/loop cycle. Figure 3(c) presents the bitmap D showing in grey levels the region with damping constant. Regions of

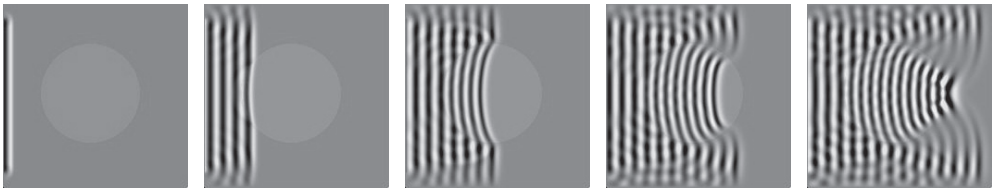

Figure 4. A sequence of snapshots showing the propagating waves in the simulated space.

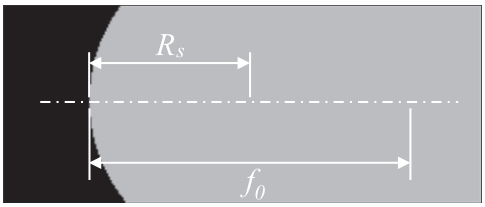

Figure 5. Bitmap M for a transparent medium having a spherical interface of radius R_s and focal distance f_0.

graded damping constant different from zero were placed in the border of the bitmap D in order to minimize the reflection of the travelling waves at the edges of the simulation space having clamped boundary conditions. Figure 4 presents a sequence of snapshots taken at different equispaced times for the simulation space defined with the set of bitmaps shown in figure 3. In sequence, it is possible to observe the travelling wavefronts and their interaction with the circular region for elapsed times of 20, 105, 190, 275 and 360 ms after the start of the simulation.

5.2. Refraction at a spherical surface

In this example, the wave focusing properties of a spherical surface are reproduced with the proposed simulation and related to the results obtained by means of geometrical optics. The refraction of a wave through this type of surface is of great importance in optics since it represents the basic principle of lens focusing and image formation. According to the laws of geometrical optics, an incident plane wave will be focused inside a transparent medium with a spherical surface of radius R_s and refractive index n_R at a focal distance f_0 from the surface given by the following expression [6]:

$$f_0 = \frac{1}{n_R - 1} R_s. \tag{19}$$

Figure 5 shows a bitmap M with a size of 840 $\times$ 345 pixels that defines a density mass distribution corresponding to the section of a spherical surface where $d = 87$ μm, which represents a real simulation space of 73 $\times$ 30 mm^2. The ground density mass was set to $\mu_0 = 1$ kg m^{-2} and the elastic constant was set to $k = 0.3$ N m^{-1}. The region in grey has a density mass $\mu = 2.25$ kg m^{-2} and it can be interpreted as a glass transparent medium having a refractive index $n_R = 1.5$. In this case, the radius R_s of the spherical interface is 20 mm, which according to (19) gives a focal distance $f_0 = 40$ mm. R_s and f_0 are indicated in figure 5.

As in the example presented in section 5.1, a plane wave travelling from the left to the right of the simulation space was generated. In this case, the frequency of harmonic excitation

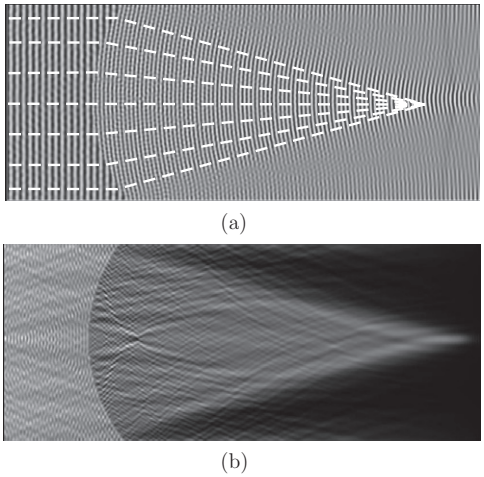

Figure 6. (a) Propagation of the waves and orthogonal lines to the wavefronts, and (b) the corresponding diagram of intensity.

was $\omega = 300$ rad s^{-1} and $\tau = 1$ ms/loop cycle. A bitmap D with a region of graded damping constant similar to that shown in figure 3(c) and with the size of the bitmap M depicted in figure 5 was also introduced to minimize the wave reflection at the edges of the simulation space. Figure 6(a) shows in grey levels the generated wavefronts for a snapshot taken 2.3 s after the start of the simulation. Figure 6(a) also shows in white a set of dashed lines that are locally orthogonal to the lines formed by the wavefronts. It can be observed that these lines correspond to the rays predicted by geometrical optics for such a structure. In addition, figure 6(b) shows the diagram of intensity, where it is possible to observe that the energy is concentrated at the focus of the system, located at a distance f_0, as expected. Since the wavelength is not negligible in relation to the size of the structure, the focus is not a well-localized spot. Because of that, the position of the focus was located more accurately by detecting the pixel of maximum intensity at this spot. In this manner, it was determined that the focal distance given by the simulation is $f_0 = 41.8$ mm, which is in good agreement with the theoretical value given by (19).

5.3. Diffraction by a single slit

In this section, the proposed simulation is applied to the study of the wave diffraction produced by a single slit. The diffraction of a wave under *the Rayleigh–Sommerfeld formulation of diffraction* [7] is described for a bidimensional space as

$$H(x, y) = -\frac{\mathrm{i}}{\lambda} \int H(0, y') \frac{\mathrm{e}^{\mathrm{i}k_w r}}{r} \cos(\theta)\, \mathrm{d}y', \tag{20}$$

where, following the notation used in this paper, H is the amplitude of the wave at the (x, y) coordinate, λ and k_w are the wavelength and wave number of the incident wave respectively, and r and $\cos(\theta)$ are defined as

$$r = \sqrt{x^2 + (y - y')^2} \tag{21}$$

and

$$\cos(\theta) = x/r. \tag{22}$$

Figure 7. Diffraction by a single slit: (a) density mass and (b) damping maps.

The intensity of the diffracted wave is calculated as

$$I(x, y) = |H(x, y)|^2. \tag{23}$$

The diffraction pattern in the region near the slit is called the *near field diffraction* or *Fresnel diffraction*, and it occurs when

$$\frac{w_s^2}{d_s \lambda} \geqslant 1, \tag{24}$$

where w_s is the width of the slit and d_s is the distance between the screen and the measurement point. On the other hand, the diffraction pattern in the far field is called *Fraunhofer diffraction*, and it occurs when

$$\frac{w_s^2}{d_s \lambda} \ll 1. \tag{25}$$

The projected intensity along a screen located in the far field can be calculated by means of the expression (20), although it can be approximated to the simpler expression [6]

$$I(\beta) = I_0 \left(\frac{\sin(\beta)}{\beta} \right)^2 \tag{26}$$

with

$$\beta = \frac{\pi w_s d_s}{\lambda r}, \tag{27}$$

where r is as defined in (21) and $x = d_s$ in this case. Figure 7(a) shows a bitmap M with a size of 525 × 390 pixels that defines a simulation space containing a wall with a single slit, with $d = 1$ mm. The slit has a width $w_s = 51$ mm and the walls forming the slit were made by setting a very high superficial density mass in relation to the ground density mass μ_0 of the medium in order to produce a very high equivalent refraction index in the walls to prevent the penetration of the waves, which will be mainly reflected. The region in black has a ground density mass $\mu_0 = 1$ kg m^{-2} and the walls have a density mass $\mu = 250$ kg m^{-2}. The elastic constant is $k = 0.3$ N m^{-1}. Figure 7(b) shows the bitmap D which is similar to that shown in figure 3(c), with the difference that in this case, high damping was also added in the region of the walls to minimize any wave travelling inside them. The bitmap E is similar to that shown in figure 3(b). The generated plane wave travelling from the left to the right of the simulation space will be transmitted through the slits producing the diffraction pattern. The frequency of the harmonic excitation was set to $\omega = 300$ rad s^{-1} and the adapting constant to $\tau = 1$ ms/loop cycle. Therefore, the wavelength of the generated wave is $\lambda = 11.5$ mm. Figure 8(a) shows in grey levels the waves transmitted through the slit for a snapshot taken 1.2 s after the start of

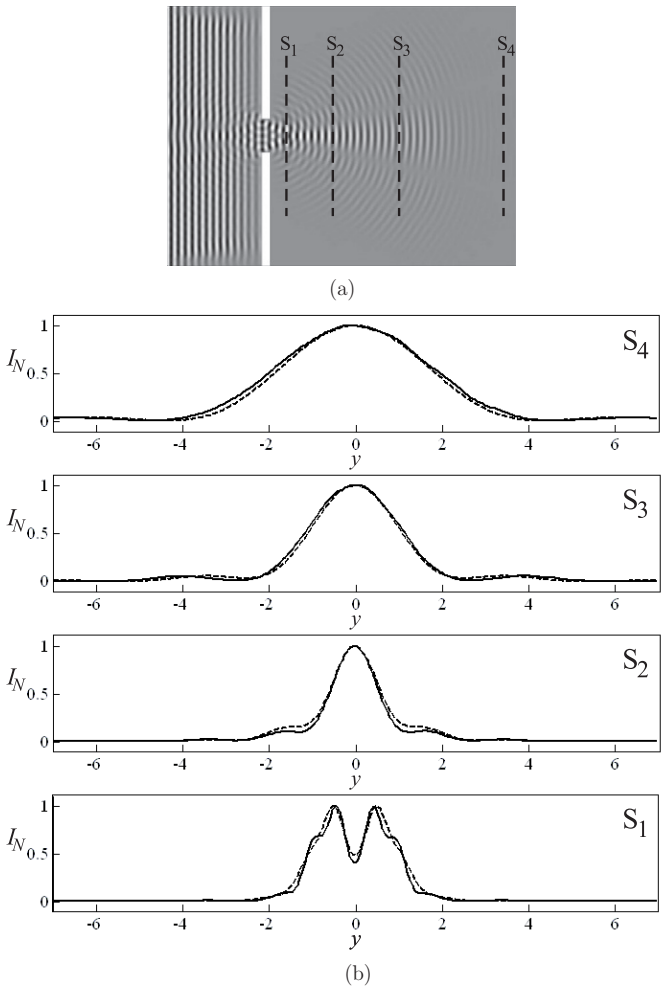

Figure 8. (a) Propagation of the waves through a single slit and four different regions of intensity measurement. (b) Normalized intensity I_N obtained by means of the simulation (solid line) and obtained theoretically (dashed line).

the simulation. The black dashed lines labelled as S_1, S_2, S_3 and S_4 and located at 25, 95, 195, 355 mm from the wall, respectively, show the regions where the intensity will be measured and they represent four different positions of a screen. According to (24) and (25), the diffraction observed over the lines S_1, S_2 and S_3 corresponds to the region of Fresnel diffraction, while the diffraction observed over the line S_4 corresponds to the region of Fraunhofer diffraction. Figure 8(b) presents the curves of normalized intensity I_N taken over the lines S_1, S_2, S_3 and S_4. The intensity obtained with the simulation is shown by the solid line, while the theoretical intensity obtained by means of (20) is shown by the dashed line. It can be observed that there is good agreement among the intensities obtained with the simulation and the intensities obtained theoretically. The slight differences between the simulated and theoretical curves may be due to the waves reflected at the edges of the simulation space that are not cancelled completely by the damping and are not considered in the theoretical calculation.

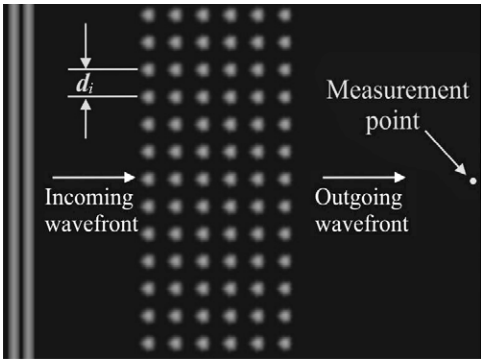

Figure 9. Structure with periodic inclusions to be analysed.

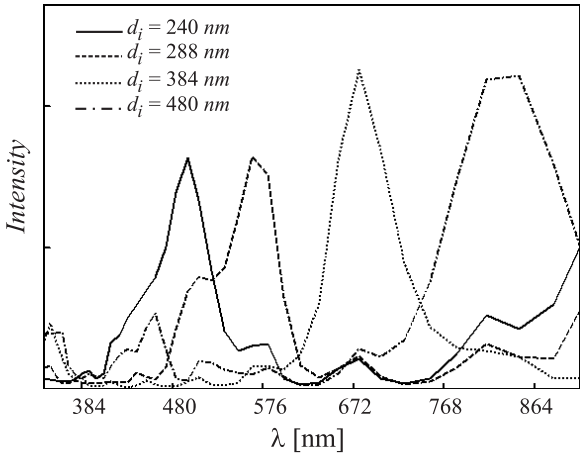

Figure 10. Spectrum of transmittance of the periodic structure for different inclusion separations.

5.4. Response to frequency of complex structures

Frequency response of complex structures is relevant in the field of photonic crystals, which are crystals with a specific refraction index distribution. The typical sizes of the regions of different refraction index are in the order of the wavelength of light and because of that, the laws of geometric optics are not suitable to analyse this kind of problem. The fabrication of photonic crystals generally aims to obtain certain transmittance spectra that result from effects of resonant scattering produced inside the structure. Due to the complexity of the structures, any analytic treatment generally becomes quite complex. Because of that, the use of simulations becomes very adequate in these types of systems.

As an example, we present here the application of the proposed approach to analyse the frequency response of a structure with a periodic refraction index distribution. Since the wave mechanics involved in dielectric optical phenomena is similar to that in mechanical waves, the response obtained in our case will be equivalent to the response that would be obtained with a similar dielectric optical structure. Figure 9 shows a bitmap M with a size of 250 $\times$ 186 pixels representing a structure consisting in a periodic arrangement of inclusions with a

refraction index $n_R = 1.65$. In this case, the separation between pixels represents a distance $d = 48$ nm and the simulation space represents a real space of 12×9 μm^2 approximately. The spectrum of transmittance of the structure to an incoming plane wave was analysed for an interval of frequencies with a wavelength ranging from 340 to 912 nm, corresponding to light waves in an interval from the near ultraviolet to the far infrared. The spectrum of transmittance of the structure was obtained by measuring the transmitted intensity at the point shown in figure 9. The separation d_i among the inclusions was of the order of the optical wavelength. Figure 10 shows the resulting transmittance spectrum for different inclusion separations d_i as a function of the wavelength of the incident wavefront obtained by exploring a set of 46 equispaced frequencies. From this figure, it is observed that there is a predominant peak of transmittance for each inclusion spacing that is shifted as the separation d_i is varied. It can also be observed that there exists a nearly linear correlation between the inclusion spacing and the transmitted wavelength.

6. Conclusion

This paper presents a very simple approach to simulate with a computer the collective movement of a bidimensional arrangement of masses joined by elastic springs. We can extrapolate the results to a continuum medium by making the arrangement of masses large enough. Although the only physical law considered in the simulation was Newton's second law and no *a priori* laws concerning wave mechanics were included, it reproduces accurately the properties of propagating waves in a continuum medium, showing the underlying connection among the wave and particle descriptions of this particular system.

Furthermore, we presented a method based on the interpretation of digital images or bitmaps that directly allows us to determine the size and shape of the medium and to 'code' its physical characteristics by means of the grey levels of the image pixels.

Several examples showing the propagation of the waves in different configurations were discussed. The analysis of the spectrum of transmittance of a structure with periodic inclusions of different refractive index was included among the examples, such as an application of the proposed approach to the field of photonics, in which this type of analysis is of great interest. It was found that there exists a nearly linear correlation between the inclusion spacing and the transmitted wavelength.

Acknowledgments

The author would like to thank the Agencia Nacional de Promoción Científica y Tecnológica and the Consejo Nacional de Investigaciones Científicas y Técnicas of Argentina for providing the financial support. The author also wishes to thank Dr Reinaldo Welti, Dr Gustavo E Galizzi and Dr Marcelo F Ciappina for their valuable comments and critical reading of the manuscript.

References

[1] Crawford F S 1968 *Berkeley Physics Course: Waves* vol 3 (New York: McGraw-Hill)
[2] Irby J H, Horne S, Hutchinson I H and Stek P C 1993 *Plasma Phys. Control. Fusion* **35** 601
[3] Delsanto P P and Scalerandi M 1998 *J. Acoust. Soc. Am.* **104** 2584
[4] Härtel H and Lüdke M 2000 *Comput. Sci. Eng.* **4** 87
[5] Dolinko A E 2008 *J. Phys. D: Appl. Phys.* **41** 205503
[6] Hecht E 1998 *Optics* 3rd edn (New York: Addison-Wesley)
[7] Goodman J W 1996 *Introduction to Fourier Optics* 2nd edn (New York: McGraw-Hill)